UDK 621.383.51
Original scientific article/Izvirni znanstveni članek

ISSN 1580-2949
MTAEC9, 56(6)607(2022)

COMPARATIVE STUDY OF THE RECOMBINANT ACTIVITY EFFECT AT THE GRAIN BOUNDARIES IN SILICON SOLAR CELLS

PRIMERJALNA ŠTUDIJA REKOMBINACIJSKEGA UČINKA NA MEJAH KRISTALNIH ZRN SILICIJEVIH SONČNIH CELIC

Bilal Djellil[1], Souad Merabet[2*], Hachemi Bouridah[1]

[1]Laboratory of the Materials Studies, Department of Electronics, University of Jijel, Jijel, Algeria
[2]Laboratory of Renewable Energy, Department of Electronics, University of Jijel, Jijel, Algeria

Prejem rokopisa – received: 2022-08-18; sprejem za objavo – accepted for publication: 2022-09-15

doi:10.17222/mit.2022.597

This work studies the effect of carrier trapping and the recombination activity at the grain boundaries in the *p*-layer of polysilicon solar cells with respect to the deposition temperature. The dependence of the grain size on the deposition temperature was studied in different samples of boron-doped low-pressure chemical vapor deposition (LPCVD) silicon deposits, conducted in a horizontal low-pressure atmospheric pressure reactor where the temperature varied over a range from 520 °C to about 605 °C. The obtained results show clear evidence of dependence on effective changes in the trapping effect as a function of the trapping density states, the doping level and the thickness dimension of the deposited layer.

Keywords: recombination current density, recombination rate, carrier lifetime, effective mobility

V članku avtorji opisujejo študijo vpliva pasti za nosilce nabojev in aktivnost njihove rekombinacije na mejah kristalnih zrn v *p*-sloju poli-silicijevih solarnih celic, v odvisnosti od temperature pri izvedbi nanosa. Avtorji so študirali vpliv temperature na velikost kristalnih zrn pri različnih vzorcih silicijevih nanosov. Postopek dopiranja Si z borom (B) so izvajali s kemijskim nizkotlačnim naparevanjem (LPCVD; angl.: low-pressure chemical vapor deposition) v horizontalnem nizkotlačnem reaktorju. Pri tem se je temperatura reaktorja spreminjala v območju med 520 °C in približno 605 °C. Rezultati študije so pokazali jasno odvisnost učinkovitosti pasti za nosilce naboja od njihove gostote, nivoja dopiranja in debeline nanosa oziroma plasti Si dopiranega z B.

Ključne besede: rekombinacija tokovne gostote, hitrost rekombinacije, čas trajanja nosilcev, učinkovitost mobilnosti

1 INTRODUCTION

In recent years, the emergence of polycrystalline silicon devices has been very beneficial for the microelectronic development. Many authors have been interested in their electrical aspects. Significantly, the modeling of charge carrier transport through these layers can be considered as one of the most frequent studies.[1–5] Polycrystalline materials consist of finite-size grain structures. The boundary between two grains is a lattice defect through which the orientation of a crystal changes.[6] Grain boundaries in polysilicon act as charge carrier migration routes; thus, a reduction of these boundaries can modify the rate of undesired traps, being one of the most significant challenges of these materials.[7] In the devices with minority carriers, such as solar cells, the conversion efficiency does not depend solely on doping concentration, crystalline quality and grain dimensions, but also, and in particular, on the recombination activity at the grain boundary.[8,9]

To provide for the design and development of such cells that can become a competitor to mono-crystalline silicon cells, we need to understand how the grain size and grain boundary affect the transport of minority carriers. Indeed, grain boundary states are among the most prevalent defects in materials, which are considered critical in controlling the carrier mobility,[10] acting as recombinant centers and therefore being a source of recombination current.[11–13] The diffusion of the dopant strongly depends on the crystal structure and detailed structure of the grain boundaries. Although these occupy only a small fraction of the volume, dopant migration along these paths can markedly influence the overall dopant diffusion in the layer. The transport modeling and recombination properties of polycrystalline silicon generally assume that all grains have the same average size.[14] Different types of polysilicon are distinguished by this significant parameter, on which the physical and electrical properties depend.[15]

Thus, this study is focused on analyzing the recombination activity and effect of trap density at the grain boundaries in polycrystalline silicon solar cells, using a widely used standard transport model[16] based on a good understanding of the carrier mobility limit at the grain boundaries.

*Corresponding author's e-mail:
smerabet@univ-jijel.dz (Souad Merabet)

2 EXPERIMENTAL PART

In this work, the effect of the characteristic parameters of three series of poly-silicon layers obtained with the LPCVD method (low-pressure chemical vapor deposition) at a low pressure (53.33 Pa) and based on the decomposition of silane (SiH_4) deposited on a single crystal with the crystallographic orientation, with thicknesses of 200 nm and 300 nm and in-situ doped with boron, has been studied as a function of the grain size. More details about the deposited layers are available in the previously published works.[17,18] The dependence of the grain size on the deposition temperature was studied in a horizontal atmospheric pressure reactor, where the temperature varied over a range from 520 °C to about 605 °C. The first series of films called *p*-layer 1, deposited at 520 °C with a thickness of 200 nm, was represented by layer 1, and the second series of films called *p*-layer 2, obtained at 605 °C with a thickness of 200 nm, was represented by layer 2. Finally, the series of films called *p*-layer 3, deposited at 605 °C with a 300 nm thickness, was represented by layer 3. The follow-up of the grain size evolution of the layers shows a variation with respect to the deposition temperature. Previous studies[19] showed that the first deposits have a large grain size equal to ≈ 80 nm, while the second and third ones have a small grain size of ≈ 40 nm. Thus, the structure of layer 1 is polycrystalline with an average grain size of about twice that of layer 2 and layer 3.

An analysis is carried out using the results obtained with a previous study[17] where the structures of the films were characterized with X-ray diffraction. X-ray spectrometry is shown in **Figure 1**.

3 MODEL

Diffusion of the carriers through the traps at the grain boundaries is formulated with the Seto Model.[16] The recombination mechanism is obtained by considering the grain boundaries as the interface where carriers diffuse and recombine, which means that the geometry of the grain (especially the grain size) and the diffusion coefficient of the grain must be considered. Therefore, the recombination speed is evaluated with Equation (1), which requires the knowledge of the interface density states and the loading state of these defects.

Generally, the S_{jg} recombination speed (m·s^{-1}) at the grain boundary is determined by the density of the effectively active interface states N_t, whose level is assumed to be centered in the middle of the forbidden gap with the following Equation (1):

$$S_{jg} = \sigma_c \cdot N_t \cdot v_{th} \tag{1}$$

where σ_c is the effective capture section (m^2), v_{th} is the thermal speed (m·s^{-1}) and N_t is the density of effectively active interface states (m^{-2}).

In the case of polysilicon, the presence of defects localized at the interface introduces trap levels in the silicon bandgap (**Figure 2**). These defects can act as traps that trap carriers temporarily before returning them to the conduction band (or valence band), altering the semiconductor's conductivity. Assuming that in the case of polycrystalline silicon, the recombinant surface considered is the grain boundary since the grain width is much lower than its height[20], the expression of life duration τ (s) is given by Equation (2):[7]

$$\frac{1}{\tau_{eff}} = \frac{1}{\tau_g} + \frac{1}{\tau_{jg}} \tag{2}$$

$$\tau_{jg} = \frac{L}{2S_{jg}} = \frac{L}{2\sigma_c N_t v_{th}} \tag{3}$$

The model was simplified for a polycrystalline material and evaluated as being composed of identical crystals with an average grain size, L (m).

Although polysilicon is a three-dimensional structure, it is sufficient to calculate its transport properties to treat the problem as a single dimension. Thus, the potential barrier height is evaluated from the model used and

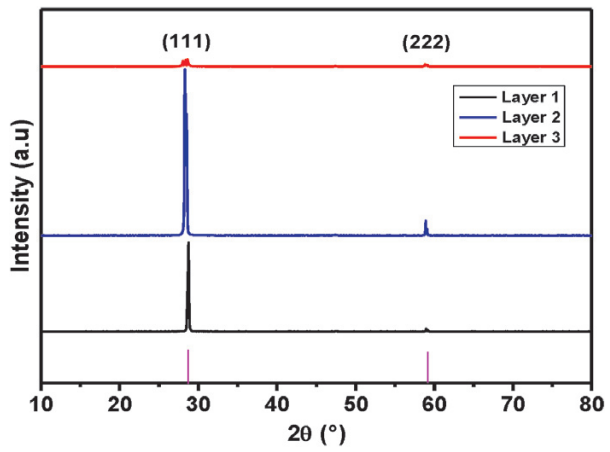

Figure 1: X-ray spectra diffraction peaks of the *p*-layers[17]

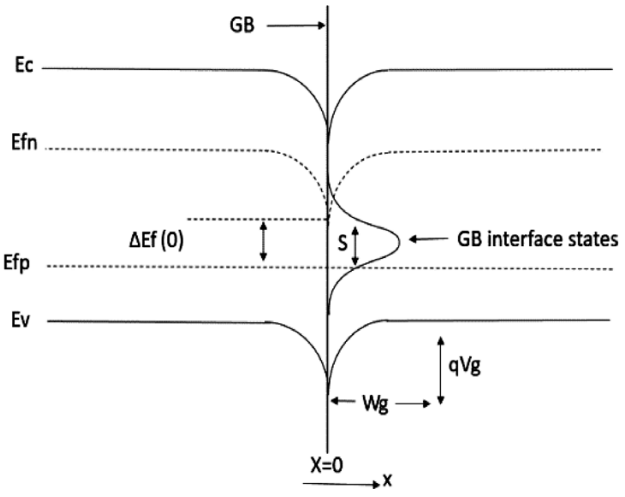

Figure 2: Energy-band diagram of *p*-type polysilicon under optical illumination

Table 1: Results obtained for the three *p*-layers

	Thickness ($\times 10^{-9}$ m)	Resistivity ($\times$ 10 Ω·m) (Ref. 17)	Trap rate N_t (m^{-2})	Critical doping concentration N^* ($\times 10^{23}$ m^{-3})	V_{bmax} (V)	V_b (V)	S_{jg} (m/s)	J_{rmax} ($\times 10^5$ A/m^2)
Layer 1	200	2.771	4.454×10^{16}	1.5	0.1736	0.00382	755.39	1.04465
Layer 2	200	3.867	9.78×10^{16}	5	0.1534	0.0164	963.0	0.23997
Layer 3	300	3.410	8.24×10^{16}	4.8	0.1506	0.0131	904.31	0.2161

another study,[21] and the recombination current density at grain boundaries is determined with Equation (4):[16]

$$J_r = qS_{jg}\left(P(0) - P_0\right) \tag{4}$$

where S_{jg} is the surface recombination rate (m·s^{-1}) at grain boundary levels, $P(0)$ is the density of minority carriers under excitation (m^{-3}), P_0 is the carrier density in equilibrium (m^{-3}) and q is the electronic charge (C).

The effective mobility μ_{eff} ($m^2 \cdot V^{-1} \cdot s^{-1}$) that describes the ease of the carrier motion from one grain to another is given by Equation (5):[16]

$$\mu_{eff} = Lq\sqrt{\frac{1}{2\pi m^* KT}} \cdot \exp\left(-\frac{E_B}{KT}\right) \tag{5}$$

where E_B is the energy potential barrier (eV) at the grain boundary, m^* is the effective mass (9.11×10^{-31} kg) of the carriers, K is the Boltzmann constant ($1\,380\,649 \times 10^{-23}$ J·K^{-1}) and T is the temperature (300 K).

4 RESULTS AND DISCUSSIONS

4.1 Recombination rate

Figure 3 shows the evolution of the recombination rate as a function of the doping level represented in the considered three layers. The obtained results show that at low levels of doping (from 1×10^{22} m^{-3} to 1×10^{24} m^{-3}), the recombination speed in the three layers is nearly the same. Then, after 1×10^{24} m^{-3} (an increase in the doping level), due to a very high doping concentration and the equivalent energy barriers of the depletion region being small, the added energy barriers at the grain boundaries will essentially limit the carrier transport.[22,23] A clear disparity between the three curves is observed due to the variation in the grain size and the recombination reaches its maximum value depending on the doping level and decreases after a certain value. The curves of layers 2 and 3 (S_{jg2max} = 936.00 m·s^{-1} at a doping of 0.67×10^{26} m^{-3} and S_{jg3max} = 904.31 m·s^{-1} at a doping of 0.54×10^{26} m^{-3}) are greater than those of layer 1 (S_{jg1max} = 755.39 m·s^{-1} at a doping of 0.38×10^{26} m^{-3}). These results are in good agreement with the previous works.[24,25]

The effect of thickness variation is observed at high doping (from 1×10^{25} m^{-3} to 6×10^{25} m^{-3}) when comparing the curves of layer 2 and layer 3. The recombination speed value of layer 3 is slightly lower than that obtained for layer 2. This can be explained with the increased thickness that led to a smaller resistivity confirmed by previous works,[17] caused by a decrease in the defect density as reported in **Table 1**.

4.2 Carrier life time

The doping of silicon (p or n) is usually above the photogeneration (a low injection rate), minority carriers are metastable and will exist, on average, only for a period equal to the lifetime. This corresponds to the average time between the electron-hole pair formation and recombination.

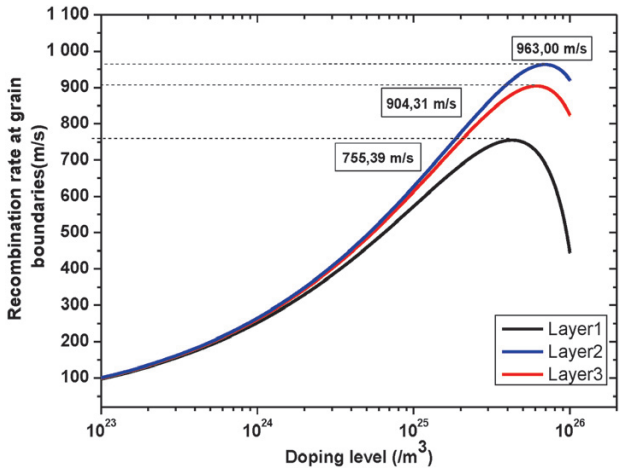

Figure 3: Recombination rate as a function of the doping level and grain size

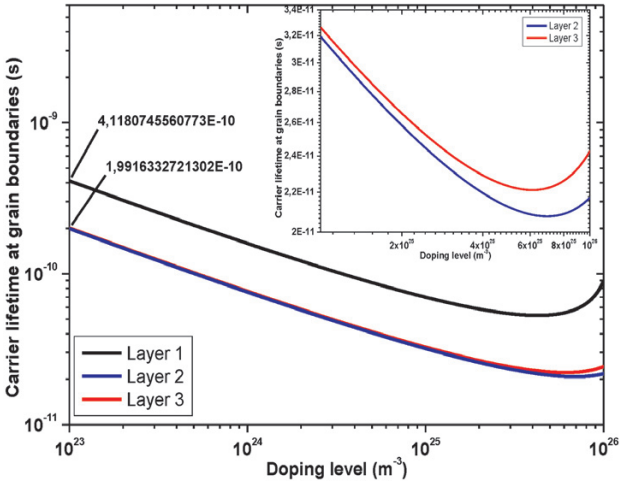

Figure 4: Carrier lifetime at grain boundaries as a function of the doping level

Figure 4 displays a linear dependence of the minority carrier lifetime at grain boundaries, which is shown to be entirely controlled by the recombination activity in the three considered layers. The evolution of the results indicates that the lifetime is proportional to the increase in the grain size and in the thickness; it is higher in layer 1 than in layers 2 and 3, and slightly lower in layer 2 with a thickness of 200 nm than in layer 3 with a thickness of 300 nm, which is in good agreement with the previous results of the recombination speed at grains boundaries.[26] The aspect of the curves also highlights that as the doping level increases the lifetime of carriers decreases up to a certain value, then the lifetime and doping level increase proportionally. This could be due to the saturation of the dangling bonds by the trapped carriers.[26]

Therefore, the concentration of the free carriers joins that of doping, and the carrier lifetime, which initially decreased, increases linearly with the dopant concentration at very high doping. These results validate those obtained for the recombination rate.

4.3 Height potential barrier and mobility

Grain boundaries contain a large number of initially neutral trap states; the dopant atoms are uniformly distributed within the grains, capturing carriers and the trap states become electrically charged, creating deserted regions and potential barriers on either side of each boundary, while the passage of free carriers from one grain to another becomes limited. The curves shown in **Figure 5** enabled the determination of the potential barrier value for the three studied layers doped with a boron concentration of $\approx 1 \times 10^{26}$ m^{-3} with respect to the change in the grain size. The potential barrier is around 0.00382 V for the films with larger grains prepared at 520 °C; it increases to 0.0164 V as the deposition temperature of the film with smaller grains is 605 °C; finally it decreases to 0.0131 V when the film thickness is increased.

In layer 1, the dopant concentration is lower than that of the trap states; the potential barrier reaches its maximum (0.1736 V) at the doping level of 1.5×10^{23} m^{-3}. The effective mobility (**Figure 6**) decreases rapidly to its lowest value at 10^{23} cm^{-3}. This is explained with the fact that almost all the carriers are trapped. As a result, the concentration of free carriers is very low and therefore the resistivity must be very high.

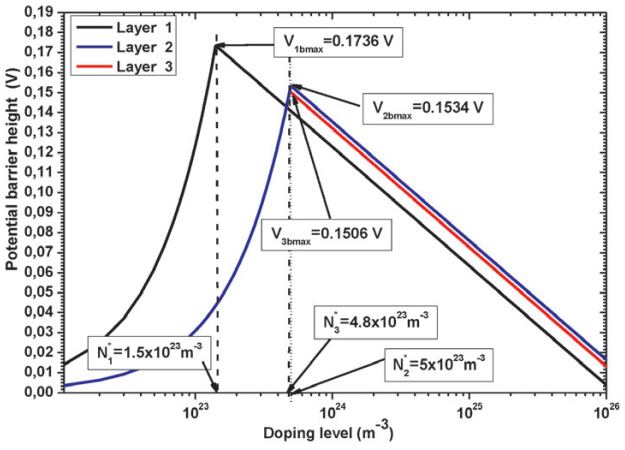

Figure 5: Potential barrier height as a function of the doping level at grain boundaries

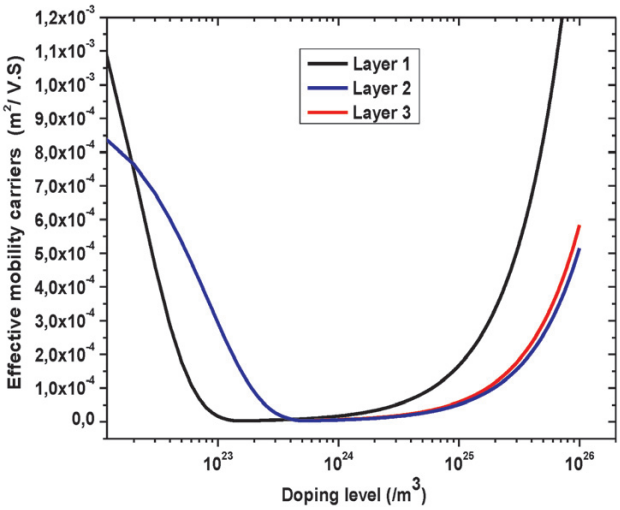

Figure 6: Effective mobility carriers as a function of the doping level at grain boundaries

Then, under the influence of a further dopant increase (10^{24} m^{-3} and more), the height of the potential barrier (**Figure 5**) decreases and the carrier effective mobility increases (**Figure 6**) due to a rapid rise in the concentration of free carriers. These results are in good agreement with other studies published in the literature.[21]

The same phenomenon was observed in the two other layers, but at a doping level equal to 5×10^{24} m^{-3}; the potential barrier reached its maximum at 0.1506 V for layer 3 and 0.1534 V for layer 2. A very small variation was noticed between the two values (the same observation at a higher doping level of carrier mobility), which could only be due to the increased thickness in layer 3, since both layers were prepared at the same deposition temperature, with practically the same average grain size.

4.4 Recombination current density

In **Figure 7**, the variation in the recombination current density in the three layers is reported. As a function of the doping level, the recombination current reaches its maximum. At a low doping level, and below the critical doping concentration N^*(m^{-3}), the concentration of free carriers is low and the resistivity is high. At the critical doping concentration $N^*_1 = 1.5 \times 10^{23}$ m^{-3} for layer 1, the recombination current density is at its maximum value equal to 1.04465×10^5 A/m^2, while for layers 2 and 3, it is 2.3997×10^6 A/m^2 and 2.161×10^6 A/m^2, obtained at critical concentrations of $N^*_2 = 5 \times 10^{23}$ m^{-3} and $N^*_3 = 4.8 \times 10^{23}$ m^{-3}, respectively (see **Table 1**).

This can be explained with the fact that the trap rate N_t (m^{-2}) at grain boundary levels differs between the

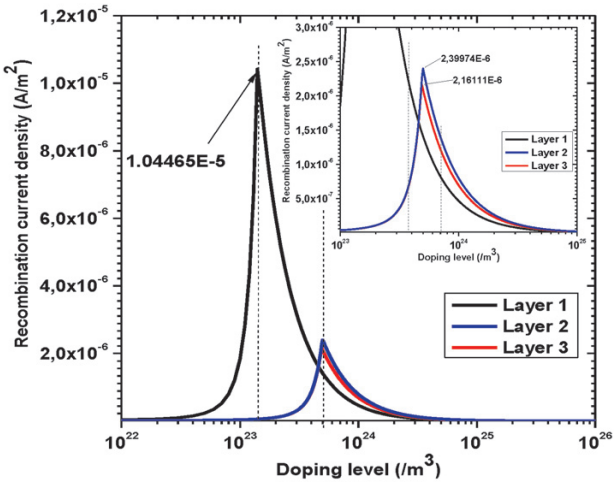

Figure 7: Recombination current density as a function of the doping level at grains boundaries

three layers. They were generated under the initial conditions of the film preparation that were verified by the experimental resistivity measurements (see **Table 1**). Beyond the critical concentration N^* (m^{-3}), when the doping concentration increases, the recombination current density decreases. At a very high doping level, both the recombination speed and the recombination current density decrease, while the carrier lifetime and mobility increase due to the saturation of the grain boundaries by the segregation phenomenon.[26,27] The grain boundaries are filled, the hanging bonds are saturated[28] and the minority carriers in this case will be able to move from the collinear grains.

The obtained results are in accord with the evolution of the deposited microstructure. At a lower deposition temperature the structure is polycrystalline with large grains, while at a higher deposition temperature it is a polycrystalline structure with small grains. Simultaneously, this leads to the appearance of a high trap density followed by carrier trapping at grain boundary levels and a decrease in the free carrier concentration.[29]

5 CONCLUSIONS

In this study, the effect of the deposit conditions and grain boundary density on the electrical parameters of three silicon layers was investigated. The results show that the structural properties and thickness have a significant impact on the photo-conductivity of the obtained films, affecting the mobility and lifetime of minority carriers. It was found that the obtained value of the recombination rate is lower for the layers with large grains prepared at a low temperature than for those with small grains prepared at a high temperature. The recombination rate is higher when the grain size is smaller.

The lifetime evolution results for the carriers show that they are completely controlled by the recombination at the grain boundaries in the three considered layers. Proportional to the increase in the thickness and grain size, the carrier lifetime is higher in layer 1 than in layers 2 and 3, and it is lower in layer 2 (with a 200-nm thickness) than in layer 3 (with a 300-nm thickness), which have the same average grain size.

The effect of the thickness variation is observed when the recombination rate values in layers 2 and 3 are compared at high doping levels (from 1×10^{25} m^{-3} to 6×10^{25} m^{-3}). The values for layer 2 are slightly higher than those obtained for layer 3.

Also, the obtained results for the potential barrier and carrier mobility showed a close dependence on the doping level and grain size. For the films with larger grains deposited at low temperatures, the critical dopant concentration N^* is lower than that for the polysilicon films deposited at slightly higher temperatures. All the results were in agreement; this was explained with the obtained structural parameters that depend on the deposition condition (deposition temperature) and the thickness size.

Acknowledgement

This work was supported by the Algerian Ministry of Higher Education and Scientific Research. We are indebted to all the members of the LME and LER Laboratories of the Jijel University for their services and technical assistance, as well as to our research teams in Jijel and Constantine. Also, we thank all the members of the LAAS Team from France for their services, and each person who has directly or indirectly contributed to the achievement of this work.

6 REFERENCES

[1] Z. Yang, Z. Liu, M. Cui, J. Sheng, L. Chen, L. Lu, W. Guo, X. Yang, Y. Zhao, W. Yang, J. C. Greer, Y. Zeng, B. Yan, J. Ye, Charge-carrier dynamics for silicon oxide tunneling junctions mediated by local pinholes, Cell Reports Physical Science, 2 (**2021**) 12, 100667, doi:10.1016/j.xcrp.2021.100667

[2] L. Galleni, M. Fırat, H. Sivarama, K. Radhakrisnan, F. Duerinckx, L. Tous, J. Poortmans, Mechanisms of charge carrier transport in polycrystalline silicon passivating contacts, J. Solar Energy Materials and Solar Cells, 232 (**2021**), 111359, doi:10.1016/j.solmat. 2021.111359

[3] D. A. Quansah, M. S. Adaramola, Comparative study of performance degradation in poly- and mono-crystalline-Si solar PV modules deployed in different applications, J. Hydrogen Energy, 43 (**2018**) 6, 3092–3109, doi:10.1016/j.ijhydene.2017.12.156

[4] G. Yoon, K. Donghoon, P. Iksoo, B. Jin, L. Jeong-Soo, Fabrication and Characterization of Nanonet-Channel LTPS TFTs Using a Nanosphere-Assisted Patterning Technique, MDP Micromachines, 12 (**2021**) 7, 741, doi:10.3390/mi12070741

[5] J. G. Min, L. Dong-Hee, K. Yeong-Ung, C. Won-Ju, Implementation of Ambipolar Polysilicon Thin-Film Transistors with Nickel Silicide Schottky Junctions by Low-Thermal-Budget Microwave Annealing, MDP Nanomaterials, 12 (**2022**) 4, 628, doi:10.3390/nano12040628

[6] J. Nomoto, K. Inaba, S. Kobayashi, T. Watanabe, H. Makino, T. Yamamoto, Characteristics of Carrier Transport and Crystallographic Orientation Distribution of Transparent Conductive Al-Doped ZnO Polycrystalline Films Deposited by Radio-Frequency, Direct-Current, and Radio-Frequency-Superimposed Direct-Current Magnetron Sputtering, MDP Materials, 10 (**2017**) 8, 916, doi:10.3390/ma10080916

[7] B. Olyaeefar, S. Ahmadi-Kandjani, A. Asgari, Classical modelling of grain size and boundary effects in polycrystalline perovskite solar cells, J. Solar Energy Materials and Solar Cells, 180 (**2018**), 76–82, doi:10.1016/j.solmat.2018.02.026

[8] K. Adamczyk, R. Søndenå, G. Stokkan, E. Looney, M. Jensen, B. Lai, M. Rinio, M. D. Sabatino, Recombination activity of grain boundaries in high-performance multicrystalline Si during solar cell processing, J. Applied Physics, 123 (**2018**), 055705, doi:10.1063/1.5018797

[9] F. Frühauf, P. P. Altermatt, T. Luka, T. Mehl, H. Deniz, O. Breitenstein, Injection intensity-dependent recombination at various grain boundary types in multicrystalline silicon solar cells, J. Solar Energy Materials and Solar Cells, 180 (**2018**), 130–137, doi:10.1016/j.solmat.2018.02.029

[10] S. K. Wallace, K. P. McKenna, Grain Boundary Controlled Electron Mobility in Polycrystalline Titanium Dioxide, Adv. Matter. Interfaces, 1 (**2014**) 5, 1400078, doi:10.1002/admi.201400078

[11] B. Gaury, P. M. Hane, Charged Grain Boundaries and Carrier Recombination in Polycrystalline Thin-Film Solar Cells, Phys. Rev. Applied, 8 (**2017**) 5, doi:10.1103/PhysRevApplied.8.054026

[12] B. H. Yan, B. Li, R. H. Yao, W. J. Wu, A physics-based effective mobility model for polycrystalline silicon thin film transistor considering discontinuous energy band at grain boundaries, Jpn. J. Appl. Phys., 50 (**2011**) 9R, 094302, doi:10.1143/jjap.50.094302

[13] A. Baumann, T. J. Savenije, D. H. K. Murthy, M. Heeney, V. Dyakonov, C. Deibel, Influence of phase segregation on the recombination dynamics in organic bulk heterojunction solar cells, Adv. Func. Mat., 21 (**2011**) 9, 1687–1692, doi:10.1002/adfm.201002358

[14] D. P. Joshi, K. Sharma, Effect of grain boundaries on the performance of polycrystalline silicon solar cells, Indian Journal of Pure and Applied Physics, 50 (**2012**) 9, 661–669

[15] B. Zaidi, B. Hadjoudja, S. Belghit, B. Chouial, M. Mekhalf, Annealing effect on grain boundary width of polycrystalline silicon for photovoltaic application, Revue des Energies Renewables, 21 (**2018**) 3, 397–401, doi:10.54966/jreen.v21i3.699

[16] J. Y. W. Seto, The electrical properties of polycrystalline silicon films, J. Appl. Phys., 46 (**1975**), 5247, doi:10.1063/1.321593

[17] S. Merabet, B. Birouk, Study of the Effect of Experimental Conditions on Polysilicon Solar Cells, J. Hydrogen Energy, 42 (**2017**) 48, 29026–29032, doi:10.1016/j.ijhydene.2017.08.070

[18] S. Merabet, A. Alioua1, B. Djellil, Effect of Deposition Conditions on Oxide Parameters of Silicon, E3S Web of Conferences, 229 (**2021**), 01037, doi:10.1051/e3sconf/202122901037

[19] D. Bielle-Daspet, E. Scheid, C. Azzaro, B. De Mauduit, B. Pieraggi, Material and electronic properties of boron-doped silicon films deposited from SiH_4-BCl_3-N_2 mixtures in an industrial low pressure chemical vapour deposition furnace, J. Thin Solid Films, 204 (**1991**) 1, 33–48, doi:10.1016/0040-6090(91)90492-G

[20] A. Trita, I. Cristiani, V. Degiorgio, Measurement of carrier lifetime and interface recombination velocity in Si–Ge waveguides, Applied Physics Letters, 91 (**2007**), 041112, doi:10.1063/1.2760133

[21] N. Gupta, B. P. Tyagi, An analytical model of the influence of grain size on the mobility and transfer characteristics of polysilicon thin-film transistors (TFTs), Physica Scripta, 71 (**2005**) 2, 225–228

[22] I. Vladimirov, M. Kühn, T. Geßner, F. May, R. T. Weitz, Energy barriers at grain boundaries dominate charge carrier transport in an electron-conductive organic semiconductor, Scientific Reports, 8 (**2018**), 14868, doi:10.1038/s41598-018-33308-y

[23] R. Gegevičius, M. Franckevičius, V. Gulbinas, The Role of Grain Boundaries in Charge Carrier Dynamics in Polycrystalline Metal Halide Perovskites, Eur. J. Inorg. Chem., (**2021**) 35, 3519–3527, doi:10.1002/ejic.202100360

[24] A. K. Ghosh, C. Fishman, T. Feng, Theory of the electrical and photovoltaic properties of polycrystalline silicon, a chapter in: Renewable Energy, 1st Edition **2011**, eBook ISBN 9781315793245

[25] D. P. Joshi, D. P. Bhatt, Grain boundary barrier heights and recombination velocities in polysilicon under optical illumination, Solar Energy Materials, 22 (**1991**) 2–3, 137–159, doi:10.1016/0165-1633(91)90013-B

[26] N. Sommer, J. Hüpkes, U. Rau, Field Emission at Grain Boundaries: Modeling the Conductivity in Highly Doped Polycrystalline Semiconductors, Phys. Rev. Appl., 5 (**2016**) 2, 024009-1–024009-22, doi:10.1103/PhysRevApplied.5.024009

[27] J. Martin, Li. Wang, L. Chen, G. S. Nolas, Enhanced Seebeck coefficient through energy-barrier scattering in PbTe nanocomposites, Phys. Rev. B, 79 (**2009**) 11, 115311, doi:10.1103/PhysRevB.79.115311

[28] L. Hyunho, L. Changhee, S. Hyung-Jun, Influence of Electrical Traps on the Current Density Degradation of Inverted Perovskite Solar Cells, Materials, 12 (**2019**) 10, 1644, doi:10.3390/ma12101644

[29] B. Ba, M. Kane, J. Sarr, Modelling recombination current in polysilicon solar cell grain boundaries, Solar Energy Materials and Solar Cells, 80 (**2003**) 2, 143–154, doi:10.1016/S0927-0248(03)00139-9